Available online at www.sciencedirect.com
SCIENCE DIRECT®
Journal of Solid State Chemistry 176 (2003) 18–26
JOURNAL OF SOLID STATE CHEMISTRY
http://elsevier.com/locate/jssc

Structures and syntheses of framework triuranyl diarsenate hydrates

Andrew J. Locock* and Peter C. Burns

Department of Civil Engineering and Geological Sciences, University of Notre Dame, 156 Fitzpatrick Hall, Notre Dame, IN 46556, USA

Received 3 March 2003; received in revised form 15 May 2003; accepted 17 May 2003

Abstract

Two homeotypic hydrated uranyl arsenates, $(UO_2)[(UO_2)(AsO_4)]_2(H_2O)_4$, *UAs*4, and $(UO_2)[(UO_2)(AsO_4)]_2(H_2O)_5$, *UAs*5 were synthesized by hydrothermal methods. Intensity data were collected at room temperature using Mo$K\alpha$ X-radiation and a CCD-based area detector. Their crystal structures were solved by direct methods and refined by full-matrix least-squares techniques on the basis of F^2 to agreement indices (*UAs*4, *UAs*5) w$R_2 = 0.116$, 0.060, for all data, and $R_1 = 0.046$, 0.033, calculated for 3176, 5306 unique observed reflections ($|F_o| > 4\sigma_F$) respectively. *UAs*4 is monoclinic, space group $P2_1/c$, $Z = 4$, $a = 11.238(1)$, $b = 7.152(1)$, $c = 21.941(2)$ Å, $\beta = 104.576(2)°$, $V = 1706.8(1)$ Å^3, $D_{calc} = 4.51$ g/cm^3. *UAs*5 is orthorhombic, space group $Pca2_1$, $Z = 4$, $a = 20.133(2)$, $b = 11.695(1)$, $c = 7.154(1)$ Å, $V = 1684.4(1)$ Å^3, $D_{calc} = 4.65$ g/cm^3. Both structures contain sheets of arsenate tetrahedra and uranyl pentagonal bipyramids, with composition $[(UO_2)(AsO_4)]^{1-}$ and the uranophane sheet anion-topology. The sheets are connected by a uranyl pentagonal bipyramid in the interlayer that shares corners with an arsenate tetrahedron on each of two adjacent sheets, resulting in open-frameworks with isolated H_2O groups in the larger cavities of the structures. The uranyl arsenate sheet in *UAs*4 is relatively planar, and is topologically identical with the uranyl phosphate sheet in $(UO_2)[(UO_2)(PO_4)]_2(H_2O)_4$. The uranyl arsenate sheet in *UAs*5 is the same geometrical isomer as in *UAs*4, but is highly corrugated, exhibiting approximately right angle bends of the sheet after every second uranyl arsenate chain repeat.

Keywords: Uranyl arsenate; Crystal structure refinement; Hydrothermal synthesis; Geometrical isomer

1. Introduction

The crystal chemistry of U^{6+} is rich in diversity [1], yet it is relatively rare for uranyl solids to form frameworks. The polarized distribution of bond strengths within uranyl bipyramidal polyhedra generally permits polymerization only through the equatorial ligands, resulting in chains or sheets. Linkages in the third dimension may be facilitated by non-uranyl polyhedra in uranyl compounds that contain additional polyhedra of higher bond-valence, such as silicate [2–4], molybdate [5,6], vanadate [7], or phosphate [8,9].

Uranyl phosphates are amongst the most abundant and widespread of uranium mineral species and together with the uranyl arsenates, constitute about one-third of the ~200 described uranium minerals. Because of their low solubilities [10], these minerals are of considerable environmental importance for understanding the mobility of uranium in natural systems [11,12], and may control the concentration of U in many groundwaters [13]. Uranyl arsenates are often structurally analogous to their chemically corresponding uranyl phosphates; cf. the isostructural mineral species abernathyite, $K[(UO_2)(AsO_4)](H_2O)_3$, and meta-ankoleite, $K[(UO_2)(PO_4)](H_2O)_3$ [14,15]. As part of our ongoing research into the structures of uranyl phosphates and uranyl arsenates, we have synthesized two closely related novel uranyl arsenate hydrates with framework structures.

2. Experiment

2.1. Crystal synthesis

Single crystals of $(UO_2)[(UO_2)(AsO_4)]_2(H_2O)_4$, *UAs*4, and $(UO_2)[(UO_2)(AsO_4)]_2(H_2O)_5$, *UAs*5, were obtained by hydrothermal reaction. The reactants (proportions listed in the order *UAs*4, *UAs*5) were $H_5As_3O_{10}$ (0.0331 g, 0.0234 g), $UO_2(NO_3)_2(H_2O)_6$ (0.1171 g, 0.1554 g), and ultrapure H_2O (4.22 mL, 5.12 mL). The

*Corresponding author. Fax: 574-247-1206.
E-mail addresses: alocock@nd.edu (A.J. Locock), pburns@nd.edu (P.C. Burns).

0022-4596/03/$ - see front matter © 2003 Elsevier Inc. All rights reserved.
doi:10.1016/S0022-4596(03)00299-8

reactants were weighed into Teflon-lined Parr autoclaves and heated at 230(1)°C—*UAs*4, and 160(1)°C—*UAs*5 in a Fisher Isotemp oven for 10 and 38 days, respectively. The autoclaves were then removed to air and allowed to cool to room temperature. The products were filtered and washed with ultrapure water, and in the case of the 230(1)°C synthesis, consisted entirely of felt-like masses of pale yellow translucent needles of *UAs*4 (determined by powder X-ray diffraction). The 160(1)°C synthesis products were determined by powder X-ray diffraction to consist dominantly of $(H_3O)[(UO_2)(AsO_4)](H_2O)_3$, with subordinate $(UO_2)[(UO_2)(AsO_4)]_2(H_2O)_4$ and trace $(UO_2)[(UO_2)(AsO_4)]_2(H_2O)_5$.

2.2. Single-crystal X-ray diffraction data collection

For both compounds, a suitable crystal was mounted on a Bruker PLATFORM three-circle X-ray diffractometer operated at 50 kV and 40 mA, and equipped with either an 1 K SMART CCD detector (*UAs*4) or a 4 K APEX CCD detector (*UAs*5), and a crystal to detector distance of ~4.7 cm. A hemisphere (*UAs*4) and a sphere (*UAs*5) of three-dimensional data were collected at room temperature using graphite-monochromatized Mo$K\alpha$ X-radiation and frame widths of 0.3° in ω, with count-times per frame of 60 s. Comparison of the intensities of equivalent reflections measured at different times during data collection showed no significant decay for either of the compounds. The unit cells (Table 1) were refined with 2675 reflections for *UAs*4, and 6585 reflections for *UAs*5 using least-squares techniques. The intensity data were reduced and corrected for Lorentz, polarization, and background effects using the Bruker program SAINT [16]. For both compounds, a semi-empirical absorption correction was applied by modeling the crystal as an ellipsoid. For *UAs*4 this procedure lowered R_{INT} of 1425 intense reflections from 0.063 to 0.038, and for *UAs*5 R_{INT} of 3714 intense reflections dropped from 0.096 to 0.058. Systematic absences of reflections for *UAs*4 were consistent only with space group $P2_1/c$. In the case of *UAs*5, systematic absences of reflections were consistent with space groups $Pca2_1$ and *Pbcm*, and assigning phases to a set of normalized structure-factors gave a mean value of $|E^2-1|$ of 0.811. Trial solutions were obtained for both space groups, but the best solution was obtained in $Pca2_1$.

Table 1
Crystallographic data and details of the structure refinements for $(UO_2)[(UO_2)(AsO_4)]_2(H_2O)_4$, *UAs*4, and $(UO_2)[(UO_2)(AsO_4)]_2(H_2O)_5$, *UAs*5

Compound	*UAs*4	*UAs*5
a (Å)	11.238(1)	20.133(2)
b (Å)	7.152(1)	11.695(1)
c (Å)	21.941(2)	7.154(1)
β (°)	104.576(2)	90
V (Å^3)	1706.8(1)	1684.4(1)
Space group	$P2_1/c$	$Pca2_1$
Analysis temperature (K)	293(2)	293(2)
Synthesis temperature (K)	503(1)	433(1)
Formula ($Z=4$)	$(UO_2)[(UO_2)(AsO_4)]_2(H_2O)_4$	$(UO_2)[(UO_2)(AsO_4)]_2(H_2O)_5$
Formula weight (g/mol)	1160.0	1178.0
Wavelength (Å)	0.71073	0.71073
$F(000)$	1976	2016
μ (mm^{-1})	32.33	32.76
D_{calc} (g/mL)	4.51	4.65
Crystal size (mm)	$0.01\times0.01\times0.26$	$0.01\times0.01\times0.26$
θ range of data collection	1.88–28.33°	2.02–34.58°
Data collected	$-12\leqslant h\leqslant14$, $-9\leqslant k\leqslant9$, $-28\leqslant l\leqslant29$	$-32\leqslant h\leqslant32$, $-18\leqslant k\leqslant18$, $-11\leqslant l\leqslant11$
Total reflections	13465	33492
Unique reflections	4394	6912
R_{int}	0.056	0.077
Unique $\lvert F_o\rvert\geqslant4\sigma_F$	3176	5306
Completeness	99.6% ($\theta=28.33°$)	98.5% ($\theta=34.58°$)
Refinement method	Full-matrix least-squares on F^2	Full-matrix least-squares on F^2
Parameters varied	189	207
R_1[a] for $\lvert F_o\rvert\geqslant4\sigma_F$	0.046	0.033
wR_2[b] all data	0.116	0.060
weighting factor a	0.0584	0.0167
Goodness of fit all data	0.95	0.87
Max. min. peaks (e/Å^3)	8.3, −2.2	2.6, −1.4

[a] $R_1=[\sum||F_o|-|F_c||]/\sum|F_o|$.
[b] $wR_2=[\sum[w(F_o^2-F_c^2)^2]/\sum[w(F_o^2)^2]]^{0.5}$, $w=1/(\sigma^2(F_o^2)+(aP)^2$, $P=1/3\max(0,F_o^2)+2/3F_c^2$.

3. Structure solution and refinement

Scattering curves for neutral atoms, together with anomalous dispersion corrections, were taken from *International Tables for X-ray Crystallography, Volume IV* [17]. The SHELXTL Version 5 series of programs [16] was used for the solution and refinement of the crystal structures.

The structure of *UAs*4 was solved in space group $P2_1/c$ using direct methods, and was refined based on F^2 for all unique data. This model refined to an agreement index (R_1) of 0.076. However, several significant electron-density peaks were present in the difference-Fourier maps at locations incompatible with additional atomic sites. Inspection of the observed and calculated structure factors showed that the most disagreeable reflections all had $F_{obs} > F_{calc}$, consistent with the presence of twinning. Further refinement of the structure model showed that the crystal was twinned by pseudo-merohedry, which involved essentially complete overlap of the diffraction patterns that corresponded to each twin component. The monoclinic cell can be transformed to a *C*-centered pseudo-orthorhombic cell with dimensions $a = 42.469$ Å, $b = 11.238$ Å, $c = 7.152$ Å, $\gamma = 90.26°$ using the matrix [−10−2/100/0−10]. The twin law [100/010/−10−1] was applied in the monoclinic setting, and the structure was refined according to published methods [18,19], resulting in a significant improvement of the agreement index. The twin scale factor refined to 0.0524(5), indicating a highly asymmetrical distribution of the twin components. The final structure model including anisotropic displacement parameters for U, As, and non-H_2O O atoms converged, and gave an agreement index (R_1) of 0.046, calculated for the 3176 observed unique reflections ($|F_o| > 4\sigma_F$). The final value of wR_2 was 0.116 for all data using the structure-factor weights assigned during least-squares refinement. In the final cycle of refinement the mean parameter shift/esd was 0.000, and the maximum peaks in the final difference-Fourier maps were 8.4 and –2.2 e/Å^3. The atomic positional parameters and displacement parameters are given in Table 2, and selected interatomic distances and angles are in Table 3. The locations of the H atoms in the unit cell were not determined.

The structure of *UAs*5 was solved in space group $Pca2_1$ using direct methods, and was refined based on F^2 for all unique data. A structure model including the racemic twin law [−100/0−10/00−1] and anisotropic displacement parameters for U, As and non-interstitial O atoms converged, and gave an agreement index (R_1) of 0.033, calculated for the 5306 observed unique reflections ($|F_o| > 4\sigma_F$). The racemic twin-component scale factor refined to 0.12(1), consistent with a highly asymmetrical distribution of the enantiomorphic components. The final value of wR_2 was 0.060 for all data using the structure-factor weights assigned during least-squares refinement. In the final cycle of refinement the

Table 2
Atomic coordinates ($\times 10^4$) and displacement parameters (Å$^2 \times 10^3$) for $((UO_2)[(UO_2)(AsO_4)]_2(H_2O)_4$

*UAs*4	x	y	z	U_{eq}	U_{11}	U_{22}	U_{33}	U_{23}	U_{13}	U_{12}
U(1)	1609(1)	2410(1)	1008(1)	14(1)	17(1)	6(1)	15(1)	0(1)	1(1)	0(1)
U(2)	2998(1)	−2585(1)	1707(1)	14(1)	15(1)	7(1)	17(1)	0(1)	1(1)	0(1)
U(3)	2236(1)	−6639(1)	−1399(1)	28(1)	24(1)	36(1)	25(1)	−2(1)	10(1)	−2(1)
As(1)	436(1)	−2601(2)	602(1)	13(1)	13(1)	9(1)	15(1)	1(1)	2(1)	−1(1)
As(2)	3808(1)	2494(2)	2301(1)	13(1)	15(1)	9(1)	14(1)	0(1)	1(1)	1(1)
O(1)	2603(11)	2282(17)	500(5)	29(3)	29(6)	37(7)	20(6)	1(5)	7(5)	4(6)
O(2)	3943(10)	−2415(17)	1179(5)	27(3)	15(5)	43(7)	22(5)	5(5)	2(5)	0(5)
O(3)	5335(10)	2352(14)	2449(5)	21(2)	21(5)	14(5)	33(6)	−4(5)	12(5)	7(4)
O(4)	126(10)	−2540(14)	−188(5)	21(2)	30(6)	19(5)	16(5)	5(4)	11(5)	−4(5)
O(5)	2041(11)	−2781(14)	2229(5)	22(2)	32(6)	9(5)	27(6)	1(4)	11(5)	3(4)
O(6)	618(11)	2559(16)	1512(5)	27(3)	33(7)	25(6)	22(5)	3(5)	7(5)	1(5)
O(7)	3279(9)	4169(14)	1754(4)	18(2)	21(6)	16(5)	15(5)	5(4)	−3(4)	−3(4)
O(8)	1351(10)	−854(14)	944(5)	25(3)	30(6)	8(5)	31(6)	−2(4)	−7(5)	0(5)
O(9)	1453(10)	−4336(14)	890(5)	25(3)	30(6)	9(5)	24(6)	6(4)	−14(5)	−1(5)
O(10)	3107(10)	676(14)	1862(5)	22(2)	25(6)	12(5)	23(5)	5(4)	−6(5)	−2(5)
O(11)	−796(12)	−2680(20)	874(6)	41(3)	29(7)	66(10)	35(7)	−9(6)	21(6)	−5(7)
O(12)	3338(12)	−7720(20)	−799(5)	50(4)	21(6)	110(14)	17(6)	1(7)	1(5)	13(8)
O(13)	3305(12)	2874(17)	2930(5)	32(3)	35(7)	39(8)	26(6)	−1(5)	16(6)	−6(6)
O(14)	1189(13)	−5490(20)	−2003(6)	48(4)	38(8)	58(10)	42(8)	16(7)	−3(7)	15(7)
OW(15)	1292(16)	−9690(20)	−1826(7)	65(5)						
OW(16)	3848(17)	−4380(30)	−1430(8)	75(5)						
OW(17)	2150(16)	−3910(20)	−709(7)	65(5)						
OW(18)	3700(20)	−1330(30)	−88(11)	111(8)						

U_{eq} is defined as one third of the trace of the orthogonalized U_{ij} tensor. The anisotropic displacement parameter exponent takes the form: $-2\pi^2[h^2a^{*2}U_{11} + \cdots + 2hka^*b^*U_{12}]$.

Table 3
Selected interatomic distances (Å) and angles (deg) for $(UO_2)[(UO_2)(AsO_4)]_2(H_2O)_4$

U(1)–O(6)	1.759(12)			As(1)–O(11)	1.640(12)
U(1)–O(1)	1.769(12)	O(6)–U(1)–O(1)	179.4(5)	As(1)–O(8)	1.671(10)
U(1)–O(4)	2.298(11)	O(6)–U(1)–O(4)	86.7(4)	As(1)–O(4)	1.681(10)
U(1)–O(9)	2.344(10)	O(6)–U(1)–O(9)	88.1(5)	As(1)–O(9)	1.697(10)
U(1)–O(8)	2.352(10)	O(6)–U(1)–O(8)	90.6(5)	⟨As(1)–O⟩	1.67
U(1)–O(7)	2.498(10)	O(6)–U(1)–O(7)	92.7(4)		
U(1)–O(10)	2.509(10)	O(6)–U(1)–O(10)	88.5(4)	O(11)–As(1)–O(4)	113.7(6)
⟨U(1)–O_{ap}⟩	1.76			O(11)–As(1)–O(8)	110.1(6)
⟨U(1)–O_{eq}⟩	2.40			O(11)–As(1)–O(9)	113.0(6)
				O(4)–As(1)–O(9)	110.3(5)
U(2)–O(2)	1.762(11)			O(8)–As(1)–O(4)	112.8(5)
U(2)–O(5)	1.763(11)	O(2)–U(2)–O(5)	179.2(5)	O(8)–As(1)–O(9)	95.7(5)
U(2)–O(3)	2.279(11)	O(2)–U(2)–O(3)	91.6(4)		
U(2)–O(7)	2.342(10)	O(2)–U(2)–O(7)	90.0(5)		
U(2)–O(10)	2.355(10)	O(2)–U(2)–O(10)	90.5(5)		
U(2)–O(8)	2.491(10)	O(2)–U(2)–O(8)	89.5(4)	As(2)–O(13)	1.640(11)
U(2)–O(9)	2.497(10)	O(2)–U(2)–O(9)	89.3(5)	As(2)–O(3)	1.668(11)
⟨U(2)–O_{ap}⟩	1.76			As(2)–O(10)	1.690(10)
⟨U(2)–O_{eq}⟩	2.39			As(2)–O(7)	1.694(10)
				⟨As(2)–O⟩	1.67
U(3)–O(14)	1.740(12)				
U(3)–O(12)	1.746(12)	O(14)–U(3)–O(12)	177.4(7)	O(10)–As(2)–O(7)	96.3(5)
U(3)–O(11)	2.261(12)	O(14)–U(3)–O(11)	93.2(6)	O(13)–As(2)–O(10)	113.4(6)
U(3)–O(13)	2.299(11)	O(14)–U(3)–O(13)	93.1(6)	O(13)–As(2)–O(3)	113.7(6)
U(3)–OW(16)	2.442(18)	O(14)–U(3)–OW(16)	91.8(7)	O(13)–As(2)–O(7)	110.1(6)
U(3)–OW(17)	2.488(16)	O(14)–U(3)–OW(17)	88.3(6)	O(3)–As(2)–O(10)	111.9(5)
U(3)–OW(15)	2.503(17)	O(14)–U(3)–OW(15)	89.1(7)	O(3)–As(2)–O(7)	110.0(5)
⟨U(3)–O_{ap}⟩	1.74				
⟨U(3)–O_{eq}⟩	2.40				

Table 4
Atomic coordinates ($\times 10^4$) and displacement parameters ($Å^2 \times 10^3$) for $(UO_2)[(UO_2)(AsO_4)]_2(H_2O)_5$

UAs5	*x*	*y*	*z*	U_{eq}	U_{11}	U_{22}	U_{33}	U_{23}	U_{13}	U_{12}
U(1)	5802(1)	1606(1)	8391(1)	14(1)	16(1)	16(1)	9(1)	−1(1)	−1(1)	−3(1)
U(2)	6483(1)	2690(1)	3399(1)	14(1)	14(1)	18(1)	9(1)	1(1)	0(1)	−3(1)
U(3)	6129(1)	6761(1)	9228(1)	26(1)	21(1)	20(1)	35(1)	−3(1)	−3(1)	5(1)
As(1)	6842(1)	3734(1)	8458(2)	13(1)	13(1)	14(1)	12(1)	−1(1)	0(1)	−1(1)
As(2)	5174(1)	1070(1)	3292(2)	13(1)	14(1)	14(1)	10(1)	−1(1)	−1(1)	−3(1)
O(1)	5053(3)	−331(4)	3490(11)	19(1)	19(3)	21(2)	18(3)	−9(3)	−6(3)	−1(2)
O(2)	6530(4)	2989(6)	6628(10)	23(2)	28(4)	26(4)	15(3)	−1(3)	−5(3)	−15(3)
O(3)	7658(2)	3972(4)	8294(12)	18(1)	15(2)	19(2)	19(3)	−4(3)	8(3)	−4(2)
O(4)	5759(3)	1353(5)	1642(10)	20(2)	26(4)	20(3)	13(3)	0(3)	−8(3)	−10(3)
O(5)	6634(3)	2774(6)	111(9)	17(1)	22(3)	22(3)	7(3)	5(2)	−1(3)	−9(3)
O(6)	7059(3)	1560(4)	3631(11)	25(2)	27(3)	21(3)	26(4)	1(3)	0(3)	0(2)
O(7)	5929(3)	3839(5)	3217(13)	26(1)	23(3)	28(3)	27(4)	2(3)	1(3)	6(2)
O(8)	5215(3)	2717(5)	8700(9)	24(2)	25(3)	22(3)	24(5)	−2(3)	5(3)	1(2)
O(9)	6435(3)	4943(5)	8739(12)	42(3)	31(3)	23(3)	73(8)	−6(4)	−15(4)	14(3)
O(10)	5613(3)	1587(5)	5150(9)	15(1)	18(3)	21(3)	7(3)	−1(2)	−6(2)	−8(3)
O(11)	6399(3)	514(5)	8134(12)	29(2)	23(3)	22(3)	42(5)	−3(3)	0(3)	5(2)
O(12)	4486(3)	1788(5)	2845(9)	24(2)	18(3)	25(3)	30(4)	−1(3)	−1(3)	6(3)
O(13)	5438(4)	6277(7)	486(12)	36(2)	38(5)	33(4)	39(5)	−2(4)	1(4)	2(4)
O(14)	6830(4)	7237(6)	7983(12)	44(2)	26(4)	44(4)	62(7)	17(4)	6(4)	4(3)
OW(15)	5616(5)	6029(8)	6201(12)	49(3)	56(6)	46(5)	44(5)	−19(4)	−28(4)	14(4)
OW(16)	6882(6)	6241(7)	1951(15)	73(3)	102(9)	33(5)	83(7)	9(5)	−53(7)	−3(5)
OW(17)	6256(6)	8373(7)	1254(14)	68(3)	103(9)	34(5)	68(7)	−21(4)	−29(6)	−17(5)
OW(18)	7427(8)	9492(8)	940(20)	97(4)						
OW(19)	6436(6)	8574(10)	4740(19)	100[a]						

U_{eq} is defined as one third of the trace of the orthogonalized U_{ij} tensor. The anisotropic displacement parameter exponent takes the form: $-2\pi^2[h^2a^{*2}U_{11} + \cdots + 2\,h\,k\,a^*b^*U_{12}]$.

[a] Value constrained during refinement.

Table 5
Selected interatomic distances (Å) and angles (°) for $(UO_2)[(UO_2)(AsO_4)]_2(H_2O)_5$

U(1)–O(11)	1.763(6)			As(1)–O(9)	1.646(6)
U(1)–O(8)	1.771(6)	O(11)–U(1)–O(8)	178.5(3)	As(1)–O(3)	1.670(5)
U(1)–O(1)	2.278(5)	O(11)–U(1)–O(1)	92.5(2)	As(1)–O(5)	1.683(7)
U(1)–O(4)	2.346(7)	O(11)–U(1)–O(4)	92.1(3)	As(1)–O(2)	1.693(7)
U(1)–O(10)	2.349(6)	O(11)–U(1)–O(10)	90.0(3)	⟨As(1)–O⟩	1.67
U(1)–O(5)	2.487(7)	O(11)–U(1)–O(5)	89.4(3)		
U(1)–O(2)	2.522(7)	O(11)–U(1)–O(2)	90.9(3)	O(3)–As(1)–O(2)	113.3(4)
⟨U(1)–O_{ap}⟩	1.77			O(3)–As(1)–O(5)	113.9(3)
⟨U(1)–O_{eq}⟩	2.40			O(5)–As(1)–O(2)	96.2(3)
				O(9)–As(1)–O(2)	110.6(4)
U(2)–O(7)	1.752(6)			O(9)–As(1)–O(3)	110.8(3)
U(2)–O(6)	1.766(6)	O(7)–U(2)–O(6)	178.1(3)	O(9)–As(1)–O(5)	111.3(4)
U(2)–O(3)	2.290(5)	O(7)–U(2)–O(3)	88.7(2)		
U(2)–O(2)	2.338(7)	O(7)–U(2)–O(2)	89.1(3)		
U(2)–O(5)	2.373(7)	O(7)–U(2)–O(5)	88.6(3)		
U(2)–O(4)	2.480(6)	O(7)–U(2)–O(4)	94.1(3)	As(2)–O(12)	1.650(6)
U(2)–O(10)	2.510(6)	O(7)–U(2)–O(10)	89.2(3)	As(2)–O(1)	1.662(5)
⟨U(2)–O_{ap}⟩	1.76			As(2)–O(4)	1.700(7)
⟨U(2)–O_{eq}⟩	2.40			As(2)–O(10)	1.708(6)
				⟨As(2)–O⟩	1.68
U(3)–O(13)	1.751(9)				
U(3)–O(14)	1.759(7)	O(13)–U(3)–O(14)	179.3(4)	O(1)–As(2)–O(10)	111.0(3)
U(3)–O(9)	2.241(6)	O(13)–U(3)–O(9)	89.6(3)	O(1)–As(2)–O(4)	110.6(3)
U(3)–O(12)	2.323(6)	O(13)–U(3)–O(12)	91.8(3)	O(12)–As(2)–O(1)	113.3(3)
U(3)–OW(17)	2.392(8)	O(13)–U(3)–OW(17)	91.6(4)	O(12)–As(2)–O(10)	113.9(3)
U(3)–OW(16)	2.542(10)	O(13)–U(3)–OW(16)	90.2(4)	O(12)–As(2)–O(4)	110.4(3)
U(3)–OW(15)	2.547(8)	O(13)–U(3)–OW(15)	90.3(3)	O(4)–As(2)–O(10)	96.5(3)
⟨U(3)–O_{ap}⟩	1.76				
⟨U(3)–O_{eq}⟩	2.41				

mean parameter shift/esd was 0.000, and the maximum peaks in the final difference-Fourier maps were 2.6 and $-1.4\,e/Å^3$. The atomic positional parameters and displacement parameters are given in Table 4, and selected interatomic distances and angles are in Table 5. The locations of the H atoms in the unit cell were not determined. The refined solution obtained for *UAs*5 was checked with the ADDSYM algorithm in the program PLATON [20–22]; no higher symmetry was found.

4. Results

4.1. Structure description

There are three symmetrically independent U atoms in *UAs*4, each of which is part of an approximately linear $(UO_2)^{2+}$ cation. In each case, the uranyl ions are coordinated by five additional anions arranged at the equatorial positions of pentagonal bipyramids, with the uranyl O atoms at the apical positions of the bipyramids. The equatorial anions of the U(1) and U(2) polyhedra consist of O atoms, whereas the equatorial anions of the U(3) polyhedron consist of two O atoms and three H_2O groups.

The U(1) and U(2) pentagonal bipyramids share an equatorial edge, giving rise to a chain of alternating U(1) and U(2) bipyramids that is one polyhedron wide. The

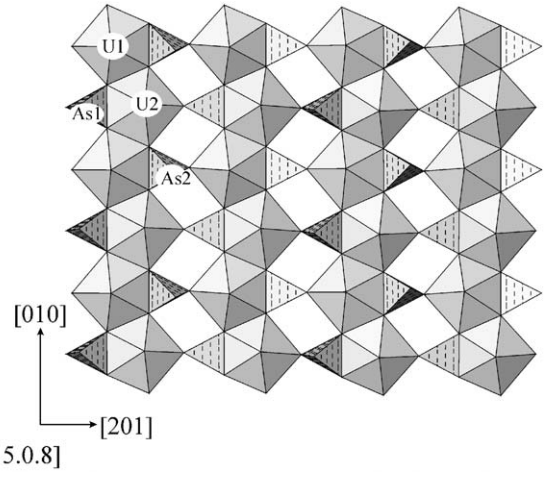

Fig. 1. Polyhedral representation of the uranyl arsenate sheet of $(UO_2)[(UO_2)(AsO_4)]_2(H_2O)_4$—*UAs*4, projected onto (−102). The sheets have the composition $[(UO_2)(AsO_4)]^{1-}$, have the uranophane sheet-anion topology, and are topologically identical with the uranyl phosphate sheets of $(UO_2)[(UO_2)(PO_4)]_2(H_2O)_4$. The uranyl polyhedra are shown in shades of gray and the arsenate tetrahedra are stippled.

arsenate tetrahedra are attached to either side of the chains by sharing edges with the uranyl polyhedra (Fig. 1). Within any uranyl arsenate chain, the orientations of all arsenate tetrahedra are identical. Translationally equivalent uranyl arsenate chains are joined by the sharing of equatorial vertices of uranyl pentagonal

bipyramids with arsenate tetrahedra from adjacent chains, resulting in planar sheets that are parallel to (−102). The uranyl arsenate sheet in *UAs*4 is topologically identical with the uranyl phosphate sheet of $(UO_2)[(UO_2)(PO_4)]_2(H_2O)_4$—*UP*4 [9], and the uranyl vanadate sheet of $(UO_2)[(UO_2)(VO_4)]_2(H_2O)_5$—*UV*5 [7].

The U(3) pentagonal bipyramid is located in the interlayer, between the uranyl arsenate sheets. Two equatorial oxygen atoms of the U(3) pentagonal bipyramid are shared with arsenate tetrahedra, linking the uranyl arsenate sheets, and resulting in an open-framework structure (Fig. 2). The coordination polyhedron about U(3) is completed by three H_2O groups, and additional H_2O groups occupy the larger cavities of the structure.

The coordination geometries and polyhedral connectivity of *UAs*5 are identical with those of *UAs*4; both structures are frameworks that consist of uranyl arsenate sheets linked by uranyl pentagonal bipyramids. However, the uranyl arsenate sheets in *UAs*5 are highly corrugated (Fig. 3), rather than planar. These sheets consist of alternating segments, two uranyl arsenate

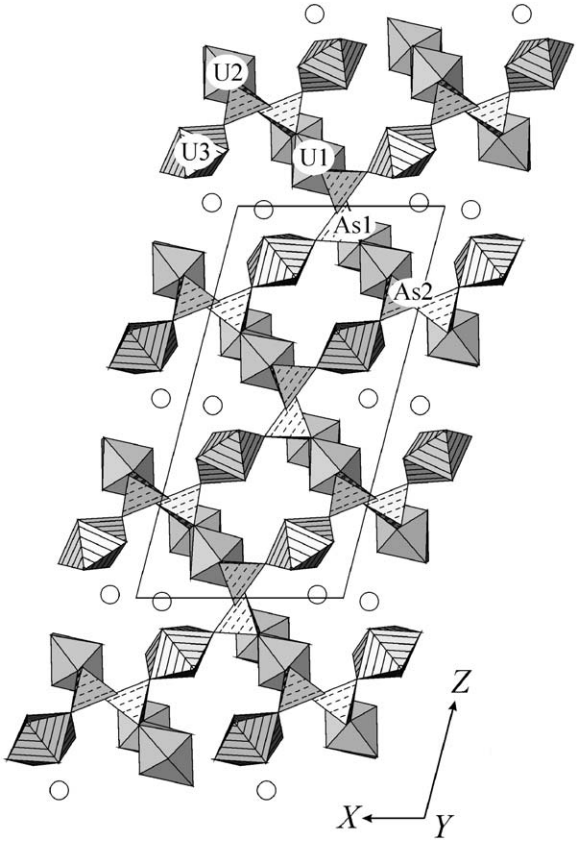

Fig. 2. Polyhedral representation of the structure of $(UO_2)[(UO_2)(AsO_4)]_2(H_2O)_4$—*UAs*4, projected along [010]. The uranyl polyhedra in the sheet are shown in shades of gray, and the uranyl polyhedra in the interlayer are striped; the arsenate tetrahedra are stippled. Interstitial H_2O groups are shown as unfilled circles.

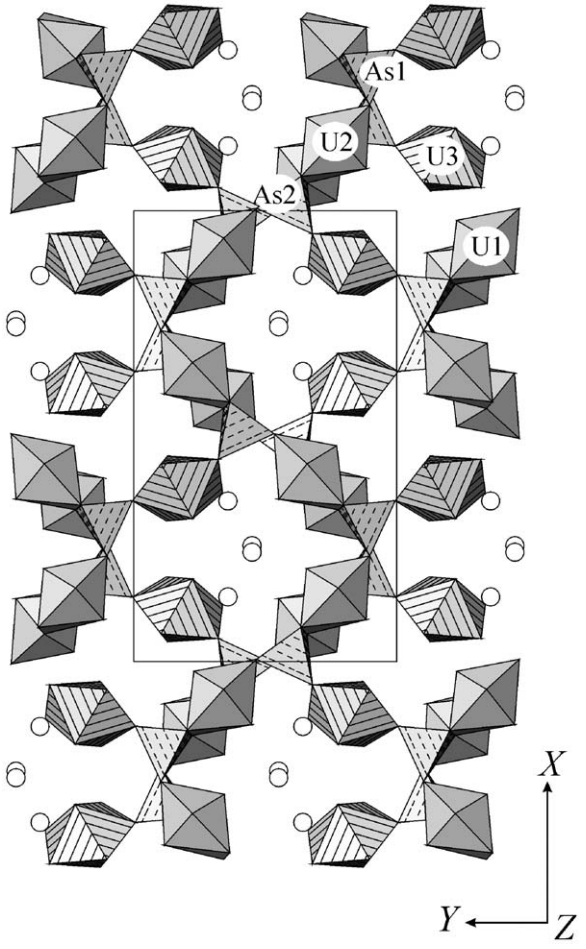

Fig. 3. Polyhedral representation of the structure of $(UO_2)[(UO_2)(AsO_4)]_2(H_2O)_5$—*UAs*5, projected along [001]. The uranyl polyhedra in the sheet are shown in shades of gray, and the uranyl polyhedra in the interlayer are striped; the arsenate tetrahedra are stippled. Interstitial H_2O groups are shown as unfilled circles.

chains wide, that are either parallel to (210) or (2−10), (Fig. 4). The acute angle between these planes is 81.4°, and the direction of chain propagation is [001].

*UAs*4, *UAs*5, *UP*4, and *UV*5 may be described as homeotypic frameworks, following the definition given in [23]. The connectivity of the uranyl polyhedra and tetrahedra (arsenate, phosphate, vanadate) are identical in all four structures, and their space groups follow supergroup–group–subgroup relations (Fig. 5).

4.2. Bond valence analysis

Bond valence analysis was performed using the parameters of Burns et al. [24] for [7] U^{6+}, and Brown and Altermatt [25] for As. For *UAs*4, the bond valence sums at the U sites are 6.00, 6.04, and 6.15 valence units for U(1), U(2), and U(3) respectively, whereas the sums at the As sites are 5.17 valence units for both As(1) and As(2). These results are consistent with formal valences of U^{6+} and As^{5+}. The bond valence sums for OW(15) to

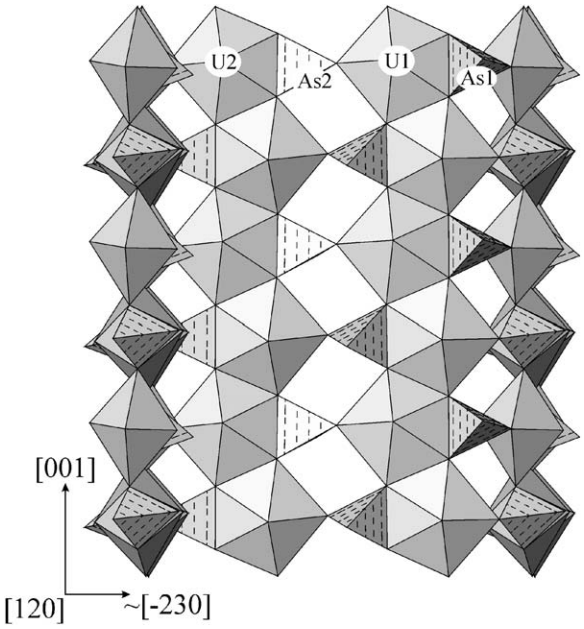

Fig. 4. Polyhedral representation of the uranyl arsenate sheet of $(UO_2)[(UO_2)(AsO_4)]_2(H_2O)_5$—*UAs*5, projected along [120]. The heavily corrugated sheets have the composition $[(UO_2)(AsO_4)]^{1-}$, and consist of alternating segments, two uranyl arsenate chains wide, that are either parallel to (210) or [2−10]. They are the same geometrical isomer as the uranyl arsenate sheets of *UAs*4. The uranyl polyhedra are shown in shades of gray and the arsenate tetrahedra are stippled.

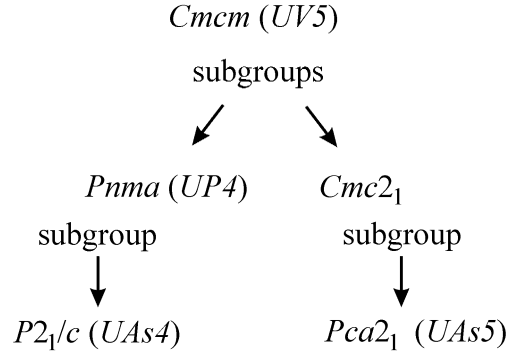

Fig. 5. Supergroup-group-subgroup relationships of the homeotypic frameworks of $(UO_2)[(UO_2)(VO_4)]_2(H_2O)_5$—*UV*5 [7], $(UO_2)[(UO_2)(PO_4)]_2(H_2O)_4$—*UP*4 [9], $(UO_2)[(UO_2)(AsO_4)]_2(H_2O)_4$—*UAs*4, and $(UO_2)[(UO_2)(AsO_4)]_2(H_2O)_5$—*UAs*5.

OW(18) range from 0 to 0.46 valence units, consistent with their assignment as H_2O groups. The bond valence sums for the remaining O atoms range from 1.72 to 2.26 valence units.

For *UAs*5, the bond valence sums at the U sites are 6.00, 6.04, and 6.05 valence units for U(1), U(2), and U(3), respectively, whereas the sums at the As sites are 5.16 and 5.07 valence units for As(1) and As(2) respectively. These results are consistent with formal valences of U^{6+} and As^{5+}. The bond valence sums for OW(15) to OW(19) range from 0 to 0.51 valence units, consistent with their assignment as H_2O groups. The bond valence sums for the remaining O atoms range from 1.71 to 2.20 valence units.

5. Discussion

5.1. Geometrical isomers of the uranophane sheet-anion topology

The uranyl arsenate sheets in *UAs*4 and *UAs*5 are based on the uranophane sheet-anion topology (Fig. 6a), which is the basis for sheets contained in several different uranyl compounds [1,26]. These sheets generally involve population of the pentagons of the underlying anion topology with uranyl ions, resulting in uranyl pentagonal bipyramids. More rarely, NaO_7 bipyramids or CaO_8 polyhedra may occupy some of these positions. In the majority of the structures, the triangular sites of the anion topology are populated by triangles or tetrahedra, with the tetrahedra oriented such that one face of the tetrahedron corresponds to the triangle in the anion topology. In a few structures, the triangle in the anion topology is vacant; in these cases, the square site is occupied by a distorted tetrahedron, or corresponds to the equatorial vertices of an octahedron [26,27].

In uranyl structures where the triangles of the uranophane sheet-anion topology are populated by tetrahedra, six different geometrical isomers [28] can be recognized on the basis of the varying orientations of the tetrahedra (Fig. 6, Table 6). In the uranophane-type sheet (Fig. 6b), found in uranophane, $Ca[(UO_2)(SiO_3OH)]_2(H_2O)_5$ [29], as well as six other uranyl silicates and the uranyl arsenate mineral seelite, all tetrahedra that share edges with one side of a uranyl chain point *down*, and all tetrahedra along the other side point *up*. In reference to the orientations of two adjacent uranyl chains, this geometrical isomer can be designated by the symbol du|du. Uranophane-beta, the dimorph of uranophane, has a sheet in which the tetrahedra on both sides of a uranyl chain *alternate* orientations along the chain length (Fig. 6c), yielding the geometrical isomer aa|aa. This sheet is also found in three inorganic– and two organic–inorganic uranyl phosphates. The uranyl phosphate sheet found in tetrapropylammonium uranyl phosphate (Fig. 6d), in which tetrahedra on either side of a uranyl chain vary orientations in an up–up–down or up–down–down sequence, gives the symbol $a_{uud}a_{udd}|a_{uud}a_{udd}$. In the uranyl vanadate-type sheet (Fig. 6e), which is also found in the homeotypic frameworks *UP*4, *UAs*4 and *UAs*5, all of the tetrahedra on a given uranyl chain point *down*, and all of the tetrahedra on the next chain point *up*, giving the geometrical isomer dd|uu. The sheet found in sodium uranyl phosphate is unique, in that all of the tetrahedra

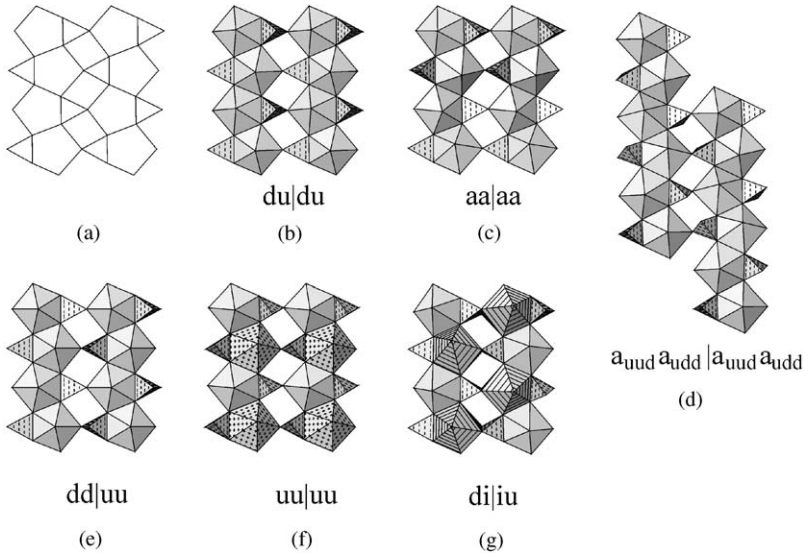

Fig. 6. Geometrical isomers of the uranophane sheet-anion topology (uranyl polyhedra are shown in gray, tetrahedra are stippled, NaO_7 pentagonal bipyramids are cross-hatched, and CaO_8 polyhedra are striped): (a) The uranophane sheet-anion topology; (b) the uranophane-type sheet, in which all tetrahedra that share edges with one side of a uranyl chain point *down*, and all tetrahedra along the other side point *up*, designation du|du; (c) the uranophane-beta-type sheet, in which tetrahedra on both sides of a uranyl chain *alternate* orientations along the chain length, designation aa|aa; (d) the sheet found in tetrapropylammonium uranyl phosphate, in which tetrahedra on either side of a uranyl chain vary orientations in an up–up–down or up–up–down sequence, designation $a_{uud}a_{udd}|a_{uud}a_{udd}$; (e) the uranyl vanadate-type sheet, in which all tetrahedra on a given uranyl chain point *down*, and all tetrahedra on the next chain point *up*, designation dd|uu; (f) the sheet found in sodium uranyl phosphate, in which all tetrahedra on all uranyl chains point *up*, designation uu|uu; (g) the ulrichite-type sheet, in which all tetrahedra on one side of a given uranyl chain point *down*, and on the other side have *intermediate* orientation (due to edge-sharing with CaO_8 polyhedra); the next chain has tetrahedra of *intermediate* orientation on the near side, and *up* pointing tetrahedra on the far side, designation di|iu.

Table 6
Geometrical isomers of the uranophane sheet-anion topology

Compound	Mineral name or *abbreviation*	Orientation of sheet	Chain direction	Geometrical isomer	Reference
$Ca[(UO_2)(SiO_3OH)]_2(H_2O)_5$	Uranophane	(100)	[010]	du|du	[29]
$K_2[(UO_2)(SiO_3OH)]_2(H_2O)_3$	Boltwoodite	(100)	[010]	du|du	[30]
$Cs_2[(UO_2)(SiO_3OH)]_2$		(100)	[010]	du|du	[31]
$Mg[(UO_2)(SiO_3OH)]_2(H_2O)_6$	Sklodowskite	(100)	[010]	du|du	[32]
$Cu[(UO_2)(SiO_3OH)]_2(H_2O)_6$	Cuprosklodowskite	(010)	[100]	du|du	[33]
$Pb[(UO_2)(SiO_4)]_2(H_2O)$	Kasolite	(100)	[010]	du|du	[34]
$Mg[(UO_2)(AsO_4)]_2(H_2O)_4$	Seelite	(100)	[010]	du|du	[35]
$Ca[(UO_2)(SiO_3OH)]_2(H_2O)_5$	Uranophane-beta	(010)	[100]	aa|aa	[36]
$K_2(UO_2)[(UO_2)(PO_4)]_4(H_2O)_2$	*KUP*	(100)	[010]	aa|aa	[37]
$Rb_2(UO_2)[(UO_2)(PO_4)]_4(H_2O)_2$	*RbUP*	(100)	[010]	aa|aa	[37]
$Cs_2(UO_2)[(UO_2)(PO_4)]_4(H_2O)_2$	*CsUP*	(100)	[010]	aa|aa	[37]
$\{(C_2H_5)_3NH\}_2[(UO_2)_2(PO_3OH)(PO_4)]$		(010)	[10−1]	aa|aa	[38]
$\{(C_2H_5)_2NH_2\}_2(UO_2)[(UO_2)(PO_4)]_4$		(010)	[10−1]	aa|aa	[8]
$\{(C_3H_7)_4N\}[(UO_2)_3(PO_3OH)_2(PO_4)]$		(0−89)	[28.−29.−26]	$a_{uud}a_{udd}\|a_{uud}a_{udd}$	[38]
$(UO_2)[(UO_2)(VO_4)]_2(H_2O)_5$	*UV*5	(100)	[001]	dd|uu	[7]
$(UO_2)[(UO_2)(PO_4)]_2(H_2O)_4$	*UP*4	(010)	[100]	dd|uu	[9]
$(UO_2)[(UO_2)(AsO_4)]_2(H_2O)_4$	*UAs*4	(−102)	[010]	dd|uu	This work
$(UO_2)[(UO_2)(AsO_4)]_2(H_2O)_5$	*UAs*5	(210), (2−10)	[001]	dd|uu	This work
$Na_{3.5}H_{0.5}[Na_2(UO_2)_3(PO_4)_4]$		(001)	[010]	uu|uu	[39]
$Cu[Ca(H_2O)_2(UO_2)(PO_4)_2](H_2O)_2$	Ulrichite	(001)	[010]	ui|id	[40]

Geometrical isomer symbols: d = downward pointing tetrahedra; u = upward pointing tetrahedra; a = alternating orientations of tetrahedra along chain length; a_{uud} = alternating orientations of tetrahedra along chain length, in sequence up–up–down; i = intermediate positioned tetrahedra.

on all uranyl chains point *up*, designation uu|uu (Fig. 6f). In the ulrichite-type sheet, all of the tetrahedra on one side of a given uranyl chain point *down*, and on the other side have *intermediate* orientations (due to edge-sharing with CaO_8 polyhedra). The next chain has tetrahedra of *intermediate* orientation on the near side for the same reason, and *up* pointing tetrahedra on the far side, and the geometrical isomer symbol is di|iu.

5.2. Frameworks

Only two of the six geometric isomers described are involved in framework structures. In the cases of *UV*5 [7], *UP*4 [9], *UAs*4 and *UAs*5, the dd|uu geometrical isomer sheets are linked to two vertices of a uranyl pentagonal bipyramid in the interlayer of each structure, resulting in relatively open frameworks. Whereas uranophane-beta-type sheets (aa|aa geometrical isomer) are linked by uranyl square bipyramids in $\{(C_2H_5)_2NH_2\}_2(UO_2)[(UO_2)(PO_4)]_4$ [8], and by uranyl pentagonal bipyramids in *CsUP*, *RbUP* and *KUP* [37], (Table 6). In each of the aa|aa cases, the uranyl polyhedron in the interlayer is linked to four phosphate polyhedra by sharing its equatorial ligands.

Acknowledgments

This research was supported by the Environmental Management Science Program of the Office of Science, US Department of Energy, Grants DE-FGO7-97ER14820 and DE-FGO7-02ER63489. AJL thanks the International Centre for Diffraction Data for the 2003 Ludo Frevel Crystallography Scholarship Award. The authors thank Robert Shuvalov, and three anonymous reviewers for their suggestions, which contributed to the improvement of the manuscript.

References

[1] P.C. Burns, M.L. Miller, R.C. Ewing, Can. Mineral. 34 (1996) 845–880.
[2] F. Demartin, C.M. Gramaccioli, T. Pilati, Acta Crystallogr. C 48 (1992) 1–4.
[3] J.M. Jackson, P.C. Burns, Can. Mineral. 39 (2001) 187–195.
[4] Y. Li, P.C. Burns, J. Nucl. Mater. 299 (2001) 219–226.
[5] S.V. Krivovichev, C.L. Cahill, P.C. Burns, Inorg. Chem. 41 (2002) 34–39.
[6] S.V. Krivovichev, P.C. Burns, Can. Mineral. 39 (2001) 207–214.
[7] M. Saadi, C. Dion, F. Abraham, J. Solid State Chem. 150 (2000) 72–80.
[8] J.A. Danis, W.H. Runde, B. Scott, J. Fettinger, B. Eichhorn, Chem. Commun. 22 (2001) 2378–2379.
[9] A.J. Locock, P.C. Burns, J. Solid State Chem. 163 (2002) 275–280.
[10] D. Langmuir, Uranium solution-mineral equilibria at low temperatures with applications to sedimentary ore deposits, in: MAC Short Course in Uranium Deposits, University of Toronto Press, Toronto, Canada, 1978, pp. 17–56.
[11] A.G. Sowder, S.B. Clark, R.A. Fjeld, Radiochim. Acta. 74 (1996) 45–49.
[12] T. Murakami, T. Ohnuki, H. Isobe, T. Sato, Am. Mineral. 82 (1997) 888–889.
[13] R.J. Finch, T. Murakami, Rev. Mineral. 38 (1999) 91–180.
[14] M. Ross, H.T. Evans, Am. Mineral. 49 (1964) 1578–1602.
[15] A.N. Fitch, M. Cole, Mater. Sci. Res. Bull. 26 (1991) 407–414.
[16] SHELXTL NT, Program Suite for Solution and Refinement of Crystal Structures, Version 5.1, Bruker Analytical X-ray Systems, Madison, WI, 1998.
[17] J.A. Ibers, W.C. Hamilton (Eds.), International Tables for X-ray Crystallography IV, Kynoch Press, Birmingham, UK, 1974.
[18] G.B. Jameson, Acta Crystallogr. A 38 (1982) 817–820.
[19] R. Herbst-Irmer, G.M. Sheldrick, Acta Crystallogr. B 54 (1998) 443–449.
[20] Y. LePage, J. Appl. Crystallogr. 20 (1987) 264–269.
[21] A.L. Spek, J. Appl. Crystallogr. 21 (1988) 578–579.
[22] A.L. Spek, PLATON, A Multipurpose Crystallographic Tool, Utrecht University, Utrecht, The Netherlands, 2001.
[23] J. Lima-de-Faria, E. Hellner, F. Liebau, E. Makovicky, E. Parthé, Acta Crystallogr. A 46 (1990) 1–11.
[24] P.C. Burns, R.C. Ewing, F.C. Hawthorne, Can. Mineral. 35 (1997) 1551–1570.
[25] I.D. Brown, D. Altermatt, Acta Crystallogr. B 41 (1985) 244–247.
[26] P.C. Burns, Rev. Mineral. 38 (1999) 23–90.
[27] S.V. Krivovichev, P.C. Burns, Can. Mineral. 38 (2000) 717–726.
[28] F.C. Hawthorne, Acta Crystallogr. A 39 (1983) 724–736.
[29] D. Ginderow, Acta Crystallogr. C 44 (1988) 421–424.
[30] P.C. Burns, Can. Mineral. 36 (1998) 1069–1075.
[31] P.C. Burns, J. Nucl. Mater. 265 (1999) 218–223.
[32] R.R. Ryan, A. Rosenzweig, Cryst. Struct. Commun. 6 (1977) 611–615.
[33] A. Rosenzweig, R.R. Ryan, Am. Mineral. 60 (1975) 448–453.
[34] A. Rosenzweig, R.R. Ryan, Cryst. Struct. Commun. 6 (1977) 617–621.
[35] B. Bachet, C. Brassy, A. Cousson, Acta Crystallogr. C 47 (1991) 2013–2015 A 1991.
[36] K. Viswanathan, O. Harneit, Am. Mineral. 71 (1986) 1489–1493.
[37] A.J. Locock, P.C. Burns, J. Solid State Chem. 167 (2002) 226–236.
[38] R.J. Francis, M.J. Drewitt, P.S. Halasyamani, C. Ranganathachar, D. O'Hare, W. Clegg, S.J. Teat, Chem. Commun. 2 (1998) 279–280.
[39] Y.E. Gorbunova, S.A. Linde, A.V. Lavrov, A.B. Pobedina, Dokl. Akad. Nauk SSSR 251 (1980) 385–389.
[40] U. Kolitsch, G. Giester, Mineral. Mag. 65 (2001) 717–724.